

Article

Disinfection of Outdoor Livestock Water Troughs: Effect of TiO₂-Based Coatings and UV-A LED

Heidi Dayana Pascagaza-Rubio ^{1,2,*}, Stéphane Godbout ², Joahnn H. Palacios ² , Dany Cinq-Mars ³,
Caroline Côté ², Alain N. Rousseau ⁴ and Sébastien Fournel ¹ 

¹ Département des sols et de Génie Agroalimentaire, Université Laval, Quebec City, QC G1V 046, Canada

² Research and Development Institute for the Agri-Environment (IRDA), Quebec City, QC G1P 3W8, Canada

³ Département des Sciences Animales, Université Laval, Quebec City, QC G1V 046, Canada

⁴ INRS-ETE/Institut National de la Recherche Scientifique-Eau Terre Environnement, 490 Rue de la Couronne, Quebec City, QC G1K 9A9, Canada

* Correspondence: heidi-dayana.pascagaza-rubio.1@ulaval.ca

Abstract: The control of pathogens is of great importance to maintaining safe water quality for animal consumption and reducing the spread of pathogens in the environment and throughout the production chain. Titanium dioxide (TiO₂) is an attractive nanoparticle for disinfection purposes because it is easy to use, highly effective under UV radiation and cost effective. The goal of this study was to assess the disinfection effectiveness of TiO₂-coated materials (high-density polyethylene, HDPE and stainless steel, SS) and UV-A LED light of non-coated materials, and the impacts of temperature and bacteria concentration in disinfection. Three TiO₂ composites, two synthesized and one commercial (namely, TiO₂, Ag-TiO₂ and P25 TiO₂), were assessed for their removal photocatalytic efficiency of methylene blue (10 mg/L). P25 TiO₂ showed fast photocatalytic efficiency after two hours of treatment, reaching 98% efficiency after 4 h. The immobilization method M1 (fast cured epoxy) of particles in the material showed the best adhesion to substrates (scale = 4 ASTM D 3359) and for TiO₂-coated stainless steel in a pre-disinfection test at a temperature of 32.3 °C and efficiency of 55.2%. There were statistically significant differences in disinfection treatments between of TiO₂-coated and non-coated materials under the influence of UV-A LED light ($p < 0.05$) at a control temperature of 26 °C. The resulting disinfection efficiencies for typical trough materials (coated (C) or non-coated (NC) HDPE; and SS) were ranked as follows: SS-C-Light (100%) > SS-Light (81.4%) > HDPE-C-Light (63.9%) > HDPE-Light (51.3%). High ambient temperature and initial bacteria concentration tended to reduce the disinfection efficiency. The presence of TiO₂ on the coated surface was confirmed using a scanning electron microscope (SEM) and energy dispersive X-ray microanalyses (EDS). These results demonstrate the disinfection potential of TiO₂-coated materials and UV-A LED light, and thus, they should be considered as valuable alternatives to deal with persistent *E. coli* contamination of cattle troughs.

Keywords: water disinfection; nanoparticles; photocatalysis; methylene blue; advanced oxidation process



Citation: Pascagaza-Rubio, H.D.; Godbout, S.; Palacios, J.H.; Cinq-Mars, D.; Côté, C.; Rousseau, A.N.; Fournel, S. Disinfection of Outdoor Livestock Water Troughs: Effect of TiO₂-Based Coatings and UV-A LED. *Water* **2022**, *14*, 3808. <https://doi.org/10.3390/w14233808>

Academic Editors: Chang-Gu Lee and Seong-Jik Park

Received: 11 October 2022

Accepted: 17 November 2022

Published: 23 November 2022

Publisher's Note: MDPI stays neutral with regard to jurisdictional claims in published maps and institutional affiliations.



Copyright: © 2022 by the authors. Licensee MDPI, Basel, Switzerland. This article is an open access article distributed under the terms and conditions of the Creative Commons Attribution (CC BY) license (<https://creativecommons.org/licenses/by/4.0/>).

1. Introduction

The presence of *Escherichia coli* (*E. coli*) O157:H7 in the cow/calf water troughs has the potential for increasing the dissemination probability of the bacteria in the animal and in the surrounding environment [1]. Different integrated management protocols for pathogen control have been implemented without successful adoption by cattle producers, such use of probiotics, antibiotics, vaccines, diet changes and source water treatment [2]. Chayer [3] evaluated the quality of source water and that of troughs of cow-calf farms located in different regions of the province of Quebec, Canada (Capitale-Nationale, Mauricie, Chaudière-Appalaches and Côte-Nord). Chayer [3] showed a water quality problem in

water troughs that was strongly related to the water temperature and *E. coli* concentration in the water, suggesting that certain types of water trough materials might be preferable to others. Commonly used materials for the construction of water troughs include: polyethylene, steel, wood, concrete and fiberglass [4]. Therefore, it appears essential to address the persistent contamination problem of not only *E. coli* at the cattle-trough level, but also of a wide variety of zoonotic waterborne pathogens threatening food safety, animal and public health and environmental quality [5].

Conventional water disinfection treatments (e.g., chlorination and UV radiation) are widely applied for the removal of a wide range of pathogens. However, these treatments are not easily applicable at the farm level and have some limitations, such as the presence of disinfection by-products, pathogens' resistance to chemical disinfection agents and bacterial regrowth [6,7]. In the search for efficient and effective treatment technologies for water disinfection, one of the options gaining interest for disinfection and removal of organic pollutants from water is the use of advanced oxidation processes (AOPs) such as photocatalysis [8,9]. This technology uses ultraviolet or even solar light for the activation of a catalyst, leading to chemical reactions [8]. The photocatalytic disinfection is based on the photoinduced e-h+ pairs. When semiconductor nanoparticles (NPs) are used as a catalyst under the influence of a radiation lamp, they are able to separate charges and form a conduction band electron to produce strong reactive oxidation species (ROS), including hydroxyl radical (HO•), hydrogen peroxide (H₂O₂) and superoxide anion (O₂•⁻) [10,11]. In the disinfection of pathogens, both HO• and O₂•⁻ are strong oxidizers that can damage the membranes of bacterial cells and destroy all types of biomolecules, such as lipids, proteins and DNA [12].

Titanium dioxide (TiO₂), including P25 TiO₂, a commercial powder of anatase/rutile mixed photocatalysis, has strong photocatalytic activity, and thus has been explored for disinfection applications. However, the application of this nanoparticle is limited by the UV range and aggregation of particles, and thus requires separation from the treated water [7].

Different methods are employed for the preparation of TiO₂ composites. Among them are co-precipitation, impregnation and sol-gel methods [13]. The sol-gel method is one of the most used methods in the synthesis of photocatalytic nanoparticles and coatings, where a precursor, a solvent and a hydrolysis agent are employed to form a suspension of gel particles [14]. To highly develop reactivity with visible light photocatalysts for water disinfection, various efforts have been made to modify TiO₂ by metal deposition (e.g., Ag and Au) [15,16]. TiO₂ nanocomposites have been used for decomposition of organic dyes such as acid blue 5 (AB5) [17], methylene blue (MB) and methyl orange (MO)—reducing them to simple inorganic species such as CO₂ and H₂O [18]. Upon MB reduction, it changes to leuco methylene blue (LMB), which is colorless [19] and easily measurable with a spectrophotometer. The similitude between chemical and biological pollutants results from the organic nature of the microorganism constituents [20], which can react with the active surface species supplied by photoactivation of NPs [21].

TiO₂ is more active when suspended than immobilized on surfaces because the close contact between the organic pollutant and TiO₂ increases the oxidative reaction [22]. However, the deposition of photocatalyst on substrates reduces: (i) the transmission of NPs to the environment, (ii) the operating cost of removal and (iii) the loss of photocatalyst [23]. The epoxy resin is one of the most important and widely used polymers because it adheres to various substrates, is chemical and solvent resistant and has low toxicity [24], yet it is stable and reusable [16]. NPs can be incorporated into a polymer's surface by: (i) chemical synthesizers; (ii) physical adsorption by non-covalent interaction, giving rise to self-assembled structures; (iii) surface reaction from a film-forming precursor; or (iv) directly incorporated into a resin [25]. The dispersed NPs as TiO₂ nanocomposites in the epoxy coating can enhance antimicrobial properties [24,26] for Gram-positive and Gram-negative bacteria killing [16]. The use of resin could be an alternative to coating with catalyst particles on plates [16].

The objective of this study was to evaluate the potential of typical trough materials (stainless steel, SS; high-density polyethylene, HDPE) coated with a TiO₂ composite for disinfection purposes (Figure 1). The photocatalytic potential of TiO₂ composites and methods of immobilization of the particles were initially evaluated for the removal of methylene blue (MB). Three TiO₂ composites (TiO₂, Ag-TiO₂, P25 TiO₂) were evaluated, including one with the incorporation of silver to determine if there was high reactivity under the influence of light. Three immobilization methods (see Section 2.3 for a complete description) of particles on trough materials were assessed, of which the two with the best photocatalytic potential were assessed in a pre-disinfection test. The TiO₂-coated materials (TiO₂ composite + an immobilization method) and non-coated materials underwent a disinfection test. Furthermore, the effects of temperature and initial bacteria concentration on the disinfection process were determined. Finally, scanning electron microscope (SEM) and energy dispersive X-ray microanalyses (EDS) were used to identify the presence of TiO₂ composites on the coated surface.

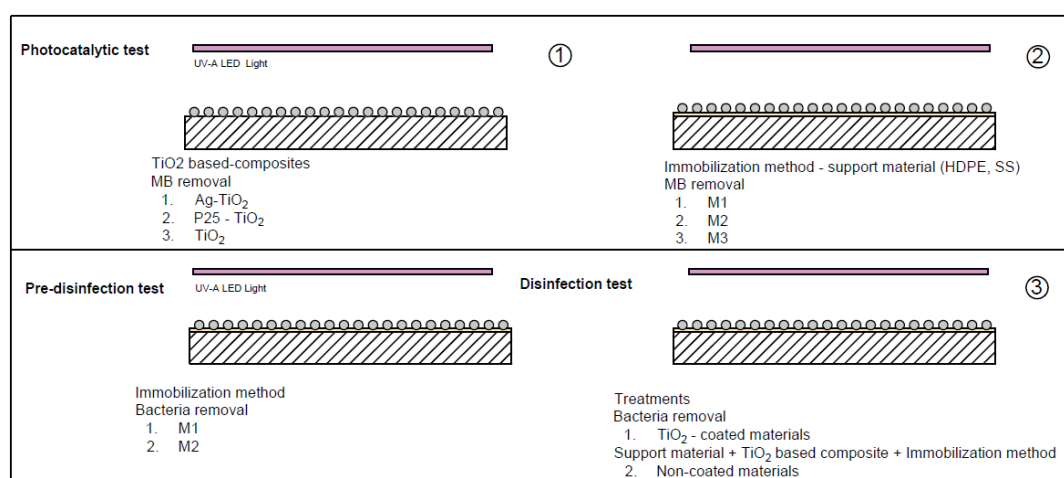


Figure 1. Experimental design scheme of each study stages. ① Evaluation of TiO₂ based-composites in the removal of MB. ② Evaluation of immobilization method on study support materials in the removal of MB. ③ Pre-disinfection test to select the most efficient immobilization method for bacteria reduction. Disinfection test to evaluate treatments (TiO₂ coated materials and non-coated materials) for bacterial removal.

2. Materials and Methods

2.1. Photocatalytic Reactor, Material Samples and Pre-Treatments

The experiment was conducted at the Research and Development Institute for the Agri-Environment (IRDA, Quebec City, QC, Canada) between June 2021 and April 2022. The setup included a reactor consisting of one dark chamber with two compartments delimited by black plastic curtains to reduce any loss of light and effects from external light. One compartment of the reactor was completely dark, irradiated with three 50 W UV-A LED blacklight floods characterized by wavelengths in the range of 365–390 nm (photocatalytic reactor), and the other one remained without any presence of light (Figure 2).

High-density polyethylene (HDPE) plates (76 mm × 76 mm) were provided by Les Revêtements Agro (Granby, QC, Canada), and stainless steel (SS) 304 plates (76 mm × 76 mm) were obtained from Ryerson (Montreal, QC, Canada). The plates were used as substrates for the formation of the TiO₂-based composites and coated materials. To increase the roughness and facilitate adhesion of the coating, HDPE plates were vigorously washed with water and detergent and rinsed with distilled water. SS plates were first degreased and cleaned using acetone; then, the plates were polished with #800 and #2000 sandpaper, and cleaned off from dust and any other impurities with acetone and rinsed with distilled water.

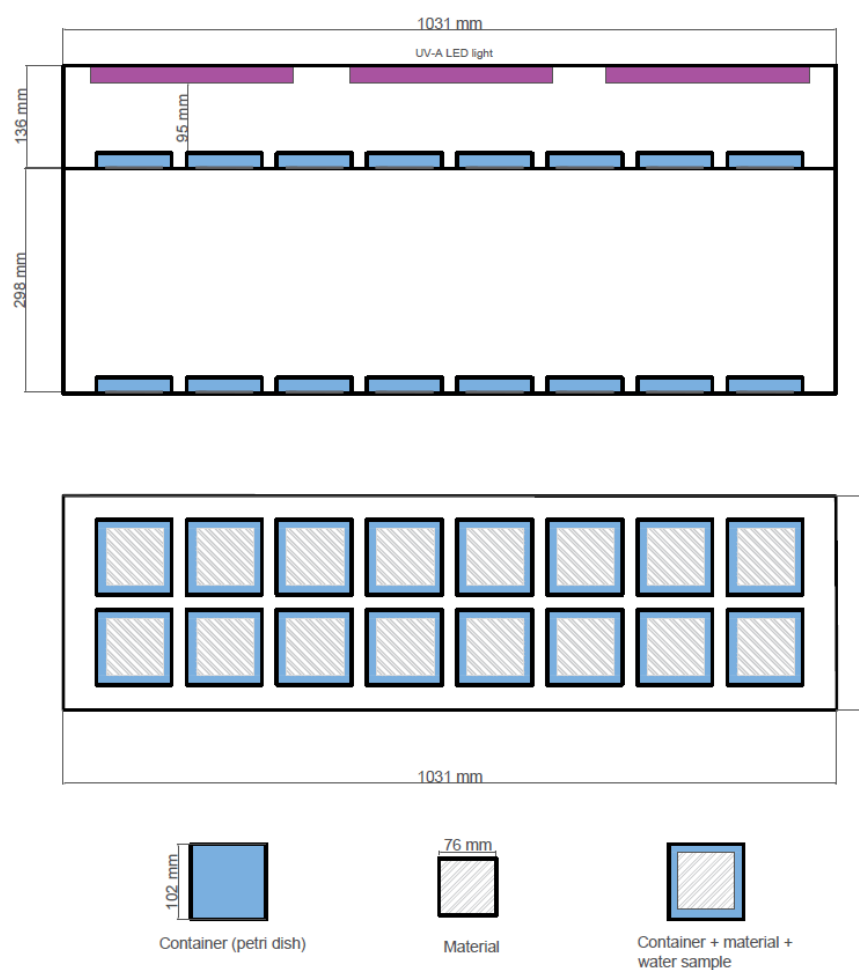


Figure 2. Scheme of the reactor used in the photocatalytic test.

2.2. Stage I. Synthesis and Photocatalytic Evaluation of TiO_2 -Based Composites

2.2.1. Synthesis

The experimental protocol was divided into three stages. The first stage focused on the efficiency of TiO_2 -based composites in the removal of a MB solution. They included commercially available NPs (P25 TiO_2 , Sigma-Aldrich, Darmstadt, Germany) and two laboratory-synthesized and heat-treated NPs (TiO_2 and Ag- TiO_2). Both NPs were produced through a sol-gel method. Silver nitrate was used as additive in the synthesis of Ag- TiO_2 [27]—in this case special attention to chemical reactions was required to avoid the risk of explosion due to the mixture of the solvent and the additive exposed to heat treatment [28].

TiO_2 and Ag- TiO_2 NPs were synthesized utilizing titanium isopropoxide 97% (TTIP) as a starting material and ethanol as solvent. Then, 15 mL of TTIP was added drop by drop to a solution prepared in a beaker by dissolving 10 g of Pluronic P-123 in 100 mL of ethanol under stirring. Then, 5 mL of acetylacetone was added to control polymerization. This solution (A) was stirred for 1 h at room temperature. Then, 1 mL of deionized water was added drop by drop to the solution. To form Ag- TiO_2 NPs, solution B was prepared by dissolving silver nitrate (AgNO_3) in ethanol to have a molar composition of Ti to Ag of 5:1. Solution B was incorporated into solution A. Then, 1 mL of deionized water was added drop by drop to the solution under stirring. The mixture was vigorously stirred for 1 h and then was sonicated using an ultrasonic cleaner bath at 40 Hz for 30 min. The precursor solutions were pre-heat treated at 120 °C for 24 h and then at 500 °C for 1 h. The ensuing material was then crushed with a mortar to obtain the fine particles [27].

To obtain a homogeneous suspension, 0.7 g each of P25 TiO₂, TiO₂ and Ag-TiO₂ each vigorously mixed with 15 mL of ethanol over 3 h. Then, the suspension was poured onto a HDPE plate as a material to support the particles and to evaluate their photocatalytic potential, without considering the influence of the support material. To obtain non-adhered films and to evaporate water and ethanol, plates were dried at 130 °C for 30 min. After natural cooling, another layer was applied. After the formation of three layers, a TiO₂-based composite supported on a HDPE plate was obtained [29].

2.2.2. Photocatalytic Evaluation

The potential photocatalytic activity of TiO₂-based composites (Ag-TiO₂, P25 TiO₂, TiO₂, Uncoated material) with three replicates per treatment was evaluated in the final MB degradation for 6 h under the influence of UV-A LED light.

The plates of TiO₂-based composites were placed in Petri dishes containing 95 mL of tap water at 10 mg/L of MB and arranged in the photocatalytic reactor under the influence of continuous light for activation of the composite for a period of 6 h.

Samples were taken at 1 h intervals to measure the remaining MB concentration with visible light adsorption intensity at 665 nm using a spectrophotometer (Eppendorf BioSpectrometer, Hamburg, Germany). The concentration of MB was calculated according to the Beer–Lambert law [21]. The photocatalytic efficiency (η ; %) was calculated as follows (Equation (1)):

$$\eta = \frac{C}{C_0} \times 100 = \frac{A}{A_0} \times 100 \quad (1)$$

where C_0 is the concentration before the reaction (mg/L) and C is the concentration every hour after the reaction has started (mg/L). A_0 is the absorbance before the reaction, and A is the absorbance obtained using the spectrophotometer every hour during the reaction.

2.3. Stage II. Immobilization Methods on Study Support Materials

A second stage was implemented to evaluate three methods of immobilization with the use of two commercially available epoxy adhesives (slow and fast cure) for the preparation of TiO₂ based-coated materials. The first method (M1) consisted in 0.5 mL of fast cure epoxy (PC-Clear, Protective Coating Company, Allentown, PA, USA) poured onto each plate and spread with a putty knife over the entire surface. ~0.2 g per plate approximately were sieved before complete hardening of the epoxy and cured in an oven at 70 °C for 24 h. In the second method (M2), NPs were spread with the help of the putty knife to create a rough surface. The third method (M3) consisted in dispersing the NPs in slow cure epoxy resin (ArtResine, Carrollton, TX, USA) with a 1:1 epoxy resin ratio and thoroughly mixed for 5 min. The mixture was poured and spread on plates and cured in an oven at 70 °C for 48 h [14]. The photocatalytic activity of the materials with TiO₂-based coatings was evaluated in the same way as described in Section 2.2.2. Then, the two most efficient immobilization methods were evaluated in a pre-disinfection test (Section 2.4.1).

TiO₂-based composite materials (HDPE-M1, SS-M1, HDPE-M2, SS-M2, HDPE-M3, SS-M3) with three replicates per treatment were assessed in the final MB degradation; that made 6 h of treatment under the influence of the UV-A LED light.

2.4. Stage III. Photocatalytic Experiments for Water Disinfection

A third stage was performed to evaluate the efficiency of the materials with TiO₂-based coatings and non-coated materials under the UV-A LED radiation during disinfection. Treatments involved coated (C) stainless steel (SS-C-Light), high-density polyethylene (HDPE-C-Light) and non-coated (NC) materials—only under the influence of UV-A LED light for stainless steel (SS-NC-Light) and high-density polyethylene (HDPE-NC-Light). Furthermore, the influences of initial bacteria concentration and temperature were evaluated in water disinfection. Gram-negative bacteria, *E. coli* (strain ATCC 8739), were used to determine their inactivation. The bacterial stock was kept at −20 °C and was inoculated in brain–heart infusion (BHI) and incubated at 37 °C to the late log phase. Then, the inoculum

was adjusted to 10^9 CFU/mL using optical density measurement until its absorbance was in the range McFarland's standard at 660 nm (0.08–0.13). The inoculum was prepared according to the absorbance [21]. Desired bacterial density was prepared by spiking of inoculum onto 95 mL of 0.9% saline solution in each Petri dish.

2.4.1. Pre-Disinfection Test

An initial disinfection pre-test was carried out to select the most efficient immobilization method for placing TiO₂-based composites on the support materials for bacteria reduction. Immobilization method 1 (M1) and method 2 (M2) were evaluated for stainless steel (SS-M1, SS-M2) and high-density polyethylene (HDPE-M1, HDPE-M2)-coated materials. First, 95 mL of a 0.9% saline solution with an initial *E. coli* concentration of 10^4 CFU/mL was transferred to the Petri dishes containing the coated materials. The Petri dishes were placed in the reactor under the influence of UV-A LED light for a period of 4.5 h. Three [3] replicates per treatment were evaluated; samples were taken at 1.5 h intervals to measure the concentration of bacteria. The average temperature during the test inside the photocatalytic reactor was 32.3 °C thanks to the heat emitted by the lamps.

2.4.2. Disinfection Test

A disinfection test was carried out using 95 mL of 0.9% saline solution to reduce the effect of osmotic stress. *E. coli* at 10^4 CFU/mL were transferred to the Petri dishes with the materials with TiO₂-based coatings under the influence of UV-A LED light (SS-C-Light, HDPE-C-Light) or the dark (SS-C-Dark, HDPE-C-Dark), and non-coated materials (SS-NC-Light, HDPE-NC-Light). The test lasted 8 h, during which, 1 mL samples were taken at 1.5 h intervals for the first six hours and after at the last 2 h to measure the concentration of bacteria and determine the inactivation level.

To circulate air along the longitudinal axis at a speed of 5 m/s, two fans (17 cm × 15 cm × 14 cm) and an icebox (AxGear, Richard, BC, Canada) were installed on the sides of the photocatalytic reactor. The ambient temperature was kept at 26 °C throughout the disinfection test to simulate the temperature of a summer field, as reported by Chayer [3].

2.4.3. Determination of the Inactivation Level

The media system for colony counting was the 3M Petrifilm *E. coli* count (EC) provided by Innovation diagnostics (3M, Sao Paulo, MN, USA). The 3M count plate is a ready-made culture medium containing modified violet red bile (VRB) nutrients, a cold-water gelling agent, and an indicator dye that facilitates counting (3M Microbiology, 2017). *E. coli* produce beta-glucuronidase and gas which generate a blue precipitate. The gas trapped around blue colonies indicates the confirmed presence of *E. coli*.

For each material disposed in a Petri dish, serial dilutions (10^1 , 10^2 , 10^3) were performed using 0.1% peptone water, and a 1 mL aliquot of each dilution was plated on the 3M Petrifilm EC. The plates were incubated for 48 h at 37 °C, and then, colonies were counted to determine the remaining bacterial concentration in the solution. Bacterial inactivation was calculated using Equation (2), dividing the concentration of bacteria in treated water (N_t) by the concentration in the feed water (N_0) before switching on the UV-A LED light:

$$\text{Log inactivation} = \text{Log} \left(\frac{N_t}{N_0} \right) \quad (2)$$

2.5. Statistical Analyses






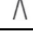
Statistical analyses were performed using R V.4.2.0 free software. One-way ANOVA was performed to test the relationships between treatments and final degradation of the study pollutant for each phase (stage I, stage II, stage III). Results with *p*-values less than 0.05 were considered statistically significant, and *p*-values less than 0.01 were considered highly significant. Followed by the LSD test, treatments with the same letter were not significantly different. Additionally, in the disinfection test, T-tests were performed to establish significant differences between treatment pairs.

2.6. Identification of TiO₂ Composite Immobilization and Adhesion Test

A coating analysis was performed to corroborate the immobilization and morphology of TiO₂ in the polymer matrix and to establish the elemental composition. The surface morphology of the coating was assessed by scanning electron microscopy (SEM), in conjunction with an energy dispersive X-ray microanalysis (EDS) to determine the composition of the material (The inspect F-50, FEI Company, Hillsboro, OR, USA). Images were obtained by scanning a surface of 1 mm × 1 mm.

Test ASTM D 3359 was performed to evaluate the adhesion of the coating to the support material. An X-cut was performed with a knife through the coating to the substrate. Pression sensitive tape was applied over the cut and then removed. The adhesion was assessed qualitatively on a 0 to 5 scale according to the detachment patterns presented in Table 1.

Table 1. Detachment patterns and classification of the coated surface after adherence test (ASTM D 3359).

Scale	Description	Pattern
0	Removal beyond the area of the X-cut	
1	Removal from most of the X-cut under the tape	
2	Jagged removal along most of the incisions up to 3.2 mm on either side	
3	Jagged removal along most of the incisions up to 1.6 mm on either side	
4	Trace peeling or removal along incisions or at their intersection	
5	No peeling removal of the coating	

3. Results and Discussion

3.1. Stage I. Photocatalytic Evaluation of TiO₂-Based Composites

Firstly, the photocatalytic activity of TiO₂-based composites (Ag-TiO₂, TiO₂, P25 TiO₂) was evaluated through the degradation of MB from an aqueous solution under UV-A LED light irradiation. Figure 3 shows the MB degradation for the TiO₂-based composites and for the control as a function of time. The concentration of MB decreased because of its decomposition in the presence of the TiO₂-based composites and the interaction of the dye with the coated surface of the plates [17]. The best photocatalytic performance was obtained for P25 TiO₂ with 98% of MB decolorization after 4 h and 99.9% within 6 h. The synthesized TiO₂ achieved an efficiency of 83% after 5 h. After 6 h of treatment, there were not any significant differences between synthesized TiO₂ and commercial P25 TiO₂. Ag-TiO₂ showed lower photocatalytic activity, with 30% MB decolorization and significant differences with respect to TiO₂-based composites without silver incorporation.

For the materials without the presence of TiO₂ composites, there was not any evidence of degradation in the concentration of MB, indicating that only light does not have any influence on the treatment. This effect has been reported in several studies of MB, where there is not any reduction in concentration without the presence of a catalyst [21,30]. However, in this study the heat emitted by the lamps induced a slight decrease in solution volume which concentrated the MB over the hours, leading to a slight increase in concentration.

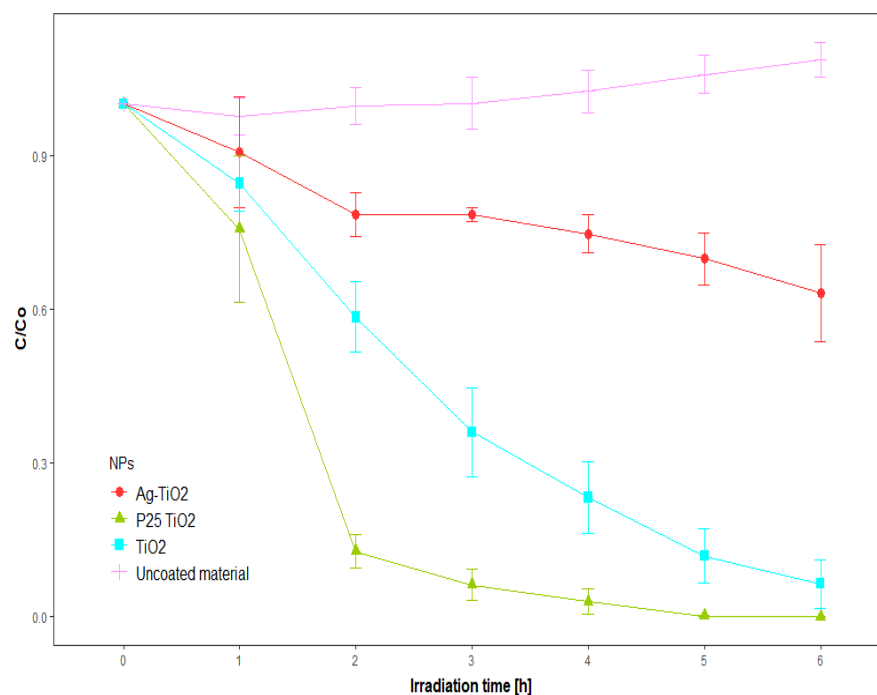


Figure 3. Degradation of the MB solution by uncoated material, Ag-TiO₂, TiO₂ and P25 TiO₂ supported on HDPE plates (n = 3).

The degradation process of P25 TiO₂ is influenced by the particle size (21 nm) and their distribution in anatase, representing about 80% of its composition, which potentiates the optimal behavior under UV light [31]. The photodegradation process becomes slow when the particle size changes by even 10 nm [32]. Dariani et al. [32] reported similar removal efficiencies of 90% in treatments for a TiO₂ of 20 nm and 70% for a particle size of 30 nm after 2 h of treatment. The particle size becomes very important as the surface area increases the contact surface between the pollutant and the catalyst [32]. In the case of this study, it is important to characterize the particle size of the synthesized TiO₂ composites to verify the assumption that they have different sizes.

Similar MB removal efficiencies for Ag-TiO₂ were reported by Montallana et al. [33], for treatment of this composite immobilized in electrospun poly (vinyl alcohol) (PVA) nanofibers with an efficiency close to 30% for two immobilization treatments using a plasma system with different etching parameters under the influence of LED light. However, other studies have reported higher photocatalytic efficiencies with the incorporation of silver compared to TiO₂; that is 25 times higher than the efficiency of P25 TiO₂ in the degradation of MB [34]. İzlen Çifçi [35] reported that an increase in Ag doping by higher than 1% (atomic ratio) results in low photocatalytic activity. Lee et al. [36] found an optimum doping percentage of 2% and higher MB reduction efficiency using UV-C lamps. Chowdhury et al. [37] reported a decrease in the efficiency of Ag-TiO₂ due to lower surface area and pore size compared to TiO₂.

The type of TiO₂ composite significantly affects ($p \leq 0.05$) the concentration of MB after 6 h of treatment (Figure 4). The efficiency of the photocatalysis process can be influenced by several parameters selected and fixed in this study, such as catalyst concentration, type of light [38], pH of water, exposure time, temperature [39] and suspension in solution or immobilization of TiO₂-based composites on support materials.

P25 TiO₂ was selected for the subsequent tests for its rapid photocatalytic effect in the reduction of MB at 2 h compared to the synthesized TiO₂ composites.

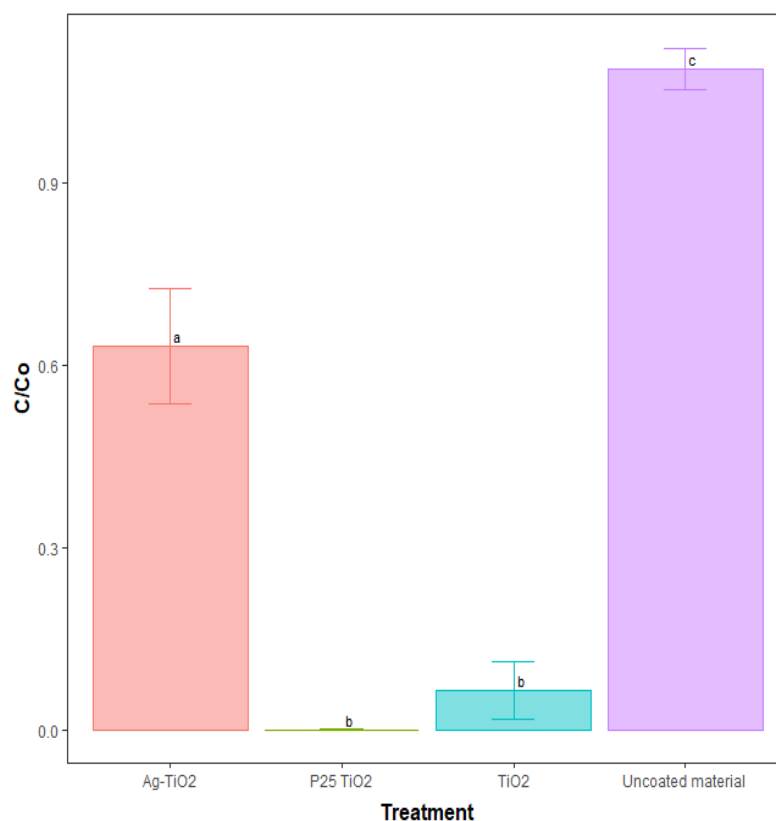


Figure 4. Remaining concentration of methylene blue (MB) after 6 h for each treatment (Ag-TiO₂, P25 TiO₂, TiO₂, uncoated material). Error bars each represent \pm standard deviation of four measurements ($n = 4$). Treatments with the same letter are not significantly different ($p > 0.05$).

3.2. Stage II. Effect of Immobilization Methods on Study Support Materials

The effect of the immobilization method of P25 TiO₂ particles on the materials was investigated for the degradation of MB. The decomposition of MB under UV-A LED light in the presence of all the P25 materials with TiO₂-based coatings is shown in Figure 5. The concentration of MB after 6 h of treatment was significantly affected ($p \leq 0.05$) by the immobilization method; however, the material did not have a significant effect ($p \geq 0.05$). MB removal efficiencies are reported in Table 2. Immobilization M2 showed the maximum MB degradation after 6 h of UV-A LED radiation for HDPE (77.2%) and SS (71.2%) as support materials. Efficiencies between 23.9% and 44.5% were achieved by immobilization M1 after 2 to 4 h of treatment, and maximum efficiencies of 58.3% and 54.4% were obtained for HDPE and SS at the end of the treatment.

Table 2. MB removal efficiencies (%) by P25 TiO₂ immobilized by three methods (M1, M2, M3) on two study materials (HDPE, SS).

Irradiation Time (hour)	MB Removal Efficiency (%)					
	M1		M2		M3	
	HDPE	SS	HDPE	SS	HDPE	SS
0	0	0	0	0	0	0
1	18.3	14.0	23.0	13.4	1.5	1.8
2	23.9	23.9	36.4	30.8	2.3	4.9
3	33.7	32.8	50.9	41.8	4.5	6.3
4	44.5	39.8	60.4	52.4	4.2	8.3
5	54.0	47.2	70.9	65.4	7.8	9.3
6	58.3	54.4	77.2	71.2	8.0	11.9

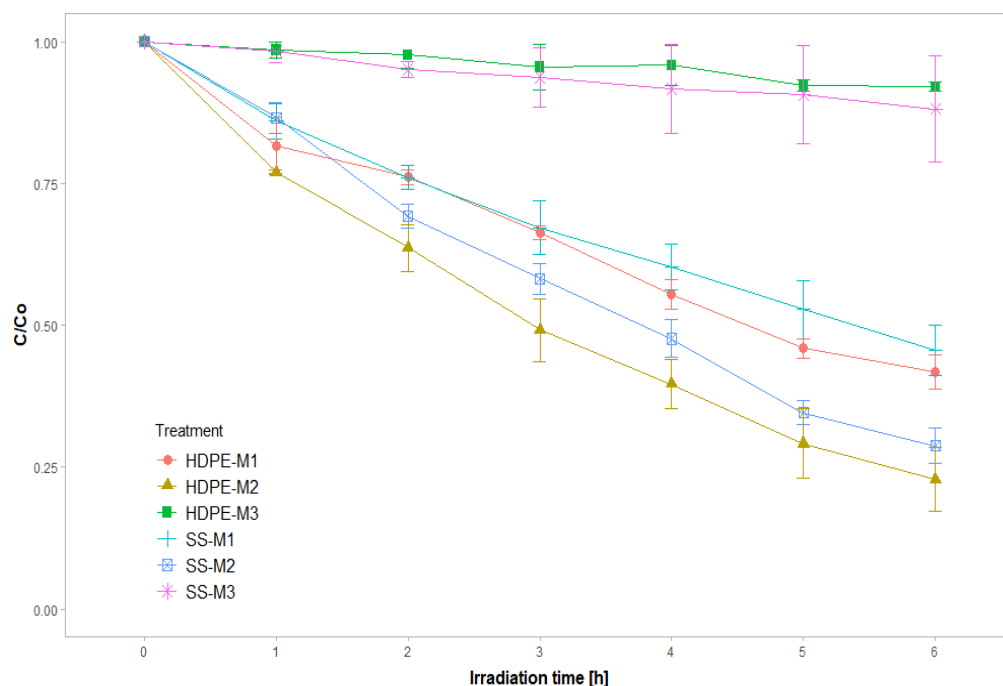


Figure 5. Degradation of the MB solution by P25 TiO₂-coated materials for immobilization methods 1 (HDPE-M1, SS- M1), 2 (HDPE-M2, SS- M2) and 3 (HDPE-M3, SS- M3) under UV-A LED radiation (n = 3).

The photocatalytic activity with respect to immobilization treatment was ranked in the following order: M2 > M1 > M3. Materials with TiO₂-based coatings after immobilization M1 and M2 revealed the best performance for the degradation of MB. The concentration of MB decreased because of its decomposition in the presence and interaction of P25 TiO₂. The lower performance of M3 may be related to the slow cure epoxy blocking the effect of particles reducing photocatalytic activity.

Similar results to those of M2 on the materials were reported for TiO₂ immobilized on polyethylene with a polyurethane resin, achieving an efficiency of 81.1% after 6 h of treatment at an optimum pH of 7.64 [40]. Yuan et al. [41] achieved 80% MB removal efficiencies with TiO₂ NPs immobilized on activated carbon fibers. Similar MB efficiencies by M1 were reported by Hussin et al. [42], who immobilized TiO₂/Zn on epoxy beads and achieved an efficiency of 27.5% MB after 2 h of treatment. The removal of other organic contaminants was evaluated on immobilized TiO₂ by using complexes with Chitosan. Shi et al. [43] reported efficiencies of 30% to 40% after 2 h of methyl orange (MO) treatment for immobilized TiO₂ (1–5 wt%) with the use of chitosan/cellulose acetate biopolymer system.

3.3. Stage III. Water Disinfection

3.3.1. Pre-Disinfection Test

The two immobilization methods of P25 TiO₂ particles that had the highest photocatalytic potential in the reduction of MB were evaluated in a disinfection pre-test.

There were not any significant differences among them (M1, M2; $p = 0.281$). Table 3 introduces the disinfection efficiencies after 4.5 h of treatment at an average temperature of 32.3 °C. For both support materials, the results suggest that M1 led to superior disinfection ability with efficiencies of 55.2% for SS and 37.9% for HDPE. Meanwhile, since M2 generated a rougher surface, it was possible that this surface created a better site for bacteria–surface interaction [44], resulting in a higher number of bacteria compared to M1. The ASTM D 3359 adhesion test was performed for the two treatments (n = 6). It was found that M1 had the best adhesion to the substrates with a score of 4A, producing slight traces of liner removal along the incisions or at their intersection, and M2 had a score of 3, assuming jagged removal along most of the incisions up to 1.6 mm on either side (Table 1).

Table 3. Bacteria removal efficiencies (%) by P25 TiO₂ immobilized by two methods (M1, M2) on the study materials (HDPE, SS) (n = 3). Initial bacteria concentration Co = 3.9 Log.

Irradiation Time (hour)	Bacteria Removal Efficiency (%)			
	M1		M2	
	HDPE	SS	HDPE	SS
0	0	0	0	0
1.5	48.9	29.9	25.5	29.4
3	46.1	32.3	26.8	22.5
4.5	37.9	55.2	12.4	9.9

3.3.2. Effect of Materials, Coatings and UV-A LED Light

As indicator of microbiological water contamination, materials with TiO₂-based coatings and the effect of light were evaluated in a disinfection test for inactivation of *E. coli* (initial bacterial concentration $\approx 1 \times 10^4$ CFU/mL) in 0.9% saline solution. The materials were made of the combination of P25 TiO₂ and M2 as the immobilization method, the most efficient components reported in the previous results.

Figure 6 illustrates the photocatalytic bacterial inactivation of the combination of P25 TiO₂ and M2 coated and non-coated materials under UV-A LED irradiation, relative to a control (dark), given the initial concentration in saline solution at a controlled temperature of 26 °C.

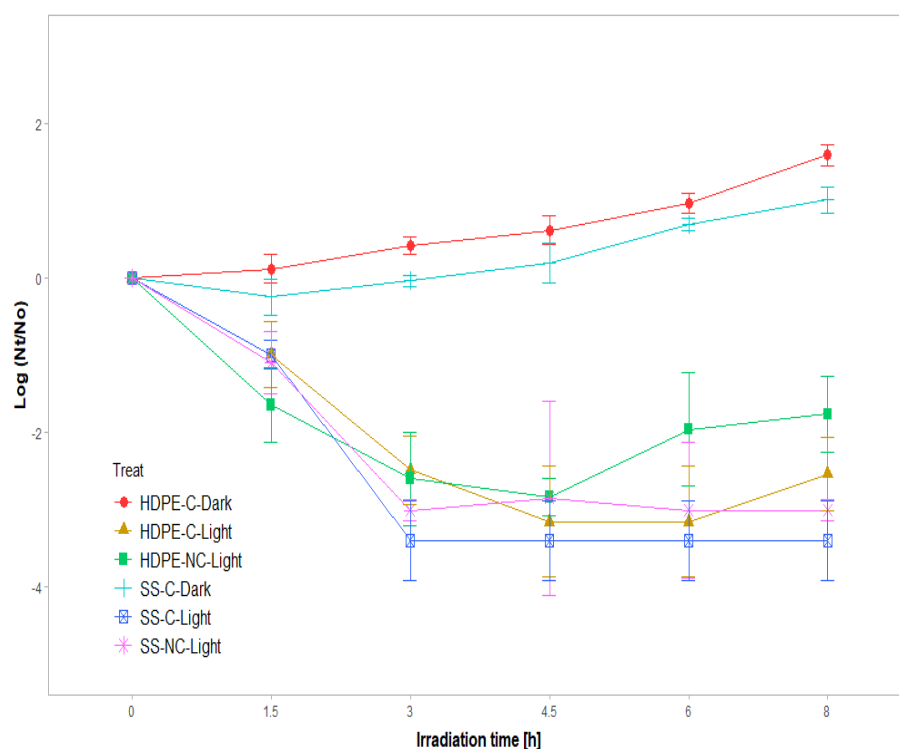


Figure 6. Degradation of *E. coli* solution by P25 TiO₂-coated materials (HDPE-C-Light, SS-C-Light) and non-coated materials (HDPE-NC-Light, SS-NC-Light) under UV-A LED radiation and coated materials in the dark (HDPE-C-Dark, SS-C-Dark) (n = 3).

Both TiO₂ based-coated and non-coated materials with the presence of UV-A LED light were able to inhibit the bacteria. The reduction in *E. coli* cells indicated that materials, given the UV-A LED exposure under the experimental conditions of this study, could inhibit the bacteria. In addition, the photocatalytic bacterial inactivation performance increased with the increase in UV irradiation time. In the absence of UV-A LED light, there was not any disinfection, which demonstrates the importance of light irradiation

in generating active species (ROS). This indeed plays an important role in the process of photocatalytic disinfection [45] by the action of light or its combination with the materials with TiO₂-based coatings.

Notably, a marked improvement in efficiency occurred from the third hour onwards. However, after 3 h, there was re-growth of bacteria for the polyethylene material with (6 h) and without coating (4.5 h). The best treatment was the stainless steel with a TiO₂-based coating, for which complete disinfection was achieved after 3 h and no regrowth was evident at the end of the test.

Similar efficiencies with TiO₂ embedded in a polymeric coating were reported by Xie et al. [46] after 3 h of treatment, achieving a near 4-log reduction of *E. coli* for a concentration of 0.8 mg/cm², and the concentration of approximately 17 mg/cm² led to a nearly 4-log reduction for SS-C-Light. The variations in efficiencies may be linked to the differences in immobilization methods, the TiO₂ concentration and the experimental setup.

The bactericidal mechanism of TiO₂ was proposed and explained by Sunada et al. [47]. It consists of two steps: a lower-rate photo-killing step and a higher-rate photo-killing step. The photo-killing step is the partial decomposition of the outer membrane by strong reactive oxygen species (ROS) produced by TiO₂. Incorporation of other compounds, such as graphitic carbon nitride [48] and silver [15] in TiO₂, has shown to improve the disinfection efficiency.

Light Effect

UVA-LED irradiation alone influences the removal of microorganisms in the water. Irradiation with UV-A light is known to induce selective oxidation of proteins and contribute to photo-inactivation, where the protein damage pattern resembles that caused by reactive oxygen stress [49]. Similarly, Lejeune et al. [50] associated direct exposure of troughs to sunlight with lower coliform and *E. coli* counts in water. However, it was shown that bacteria *E. coli* as gram negative bacteria could survive and remain infectious for an extended period [51]. Only the existence of UV light provides more chance for bacteria to exist and regrowth in the medium (Figure 6). Bacteria can repair DNA damage, even after UV inactivation, by mechanisms that occur even in the absence or presence of light [52].

There was a greater logarithmic reduction of bacteria for SS treatments than for HDPE treatments (Figure 7). The coating in the dark had no positive effect on reducing the number of bacteria, and there were not any significant differences in the growth of bacteria in the dark for TiO₂-coated materials.

Materials

There were statistically significant differences between materials. The SS-NC-Light had an efficiency higher than 30% with respect to HDPE-NC-Light in the removal of *E. coli* ($p = 0.0124$). SS-C-Light showed an efficiency higher than 48.7% with respect to SS-NC-Light ($p = 0.0014$). The bacterial community can have variations depending on the type of material and changes in water quality. Greater presence of the bacterial community for HDPE due to the possible formation of a biofilm favors the abundance of a bacterial community compared to SS [15]. Al-Ghanim et al. [53] have indicated that in plastic tanks, certain types of bacteria can adhere to the surface, allowing their growth. Similarly, Lejeune et al. [50] reported significant differences in the presence of *E. coli* in troughs of different types of materials, including a 35.5% lower amount of *E. coli* on metal compared to plastic troughs. Chayer [3] did not find any significant differences between types of trough materials; however, there was a preferable tendency to use stainless steel in comparison to other types of materials. A comparative study between materials should be carried out, comparing the characteristics of the materials and the presence of biofilm to establish their effect on disinfection.

UVA LED/TiO₂ disinfection represents an alternative, showing the potential for residual disinfection effect and energy consumption [54]. It has a better effect with steel as a support material, with which there were not any bacteria regrowth [55]. The results

indicated the following efficiency ranking at the end of the treatment (8 h) according to the LSD test results and efficiency disinfection: SS-C-Light (100%) > SS-Light (81.4%) > HDPE-C-Light (63.9%) > HDPE-Light (51.3%).

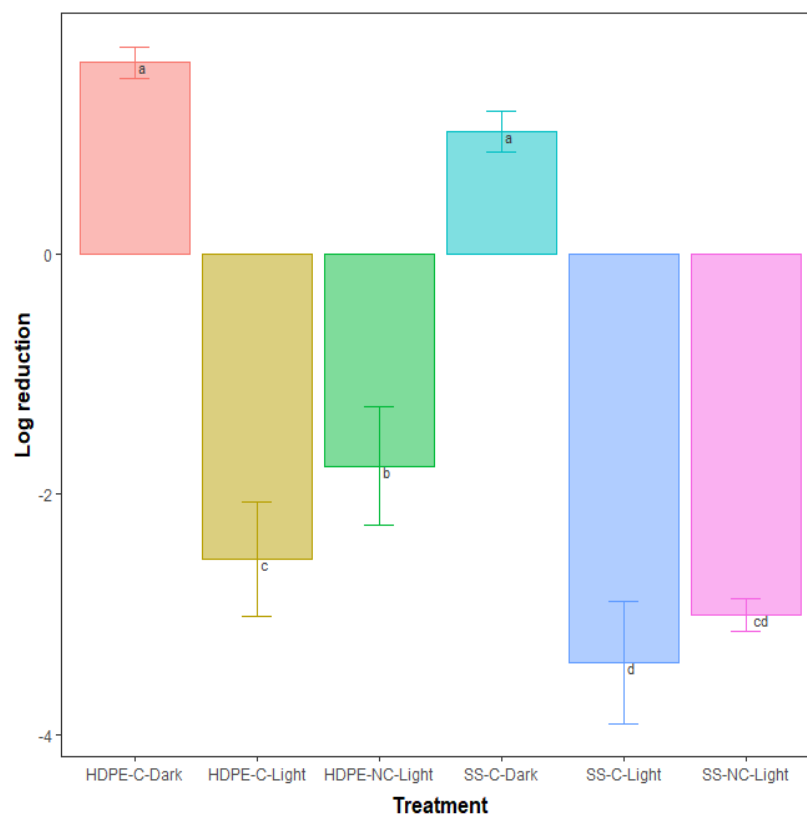


Figure 7. Logarithmic reduction of *E. coli* at 8 h of treatment by the P25 TiO₂-coated materials (HDPE-C-Light, SS-C-Light) and non-coated materials (HDPE-NC-Light, SS-NC-Light) under UV-A LED radiation, and by coated materials in the dark (HDPE-C-Dark, SS-C-Dark). Error bars represent \pm standard deviation of three measurements ($n = 3$). Treatments with the same letter are not significantly different ($p > 0.05$).

3.3.3. Effect of Bacteria Concentration

Table 4 shows the efficiencies for two groups with different initial concentrations. For the lowest concentration, the effects of light and coating on the SS caused a removal efficiency of 100% at the end of the treatment. For the HDPE, the effect of coating caused an 18.8% higher efficiency with respect to the material without coating. At the highest concentration, there was a greater effect of coating for both materials. The SS + C evidenced a higher efficiency of 18.6% with respect to the SS, and for polyethylene there was a difference of 12.6% between HDPE + C and HDPE.

Table 4. Disinfection efficiency of coated (SS + C, HDPE + C) and non-coated materials (SS, HDPE) exposed to UV-A LED light for two initial concentrations: a low concentration (10^3 CFU/mL) and a high concentration (10^4 CFU/mL).

Treatment	n	Low Concentration (log ₁₀ /mL)			High Concentration (log ₁₀ /mL)		
		Co	C	Efficiency (%)	Co	C	Efficiency (%)
SS + C	3	2.9 \pm 0.4	ND	100	4.1 \pm 0.1	ND	100
SS	3	3.0 \pm 0.2	ND	100	4.1 \pm 0.2	ND	81.4
HDPE + C	3	2.9 \pm 0.4	ND	100	4.0 \pm 0.2	1.4 \pm 1.3	63.9
HDPE	3	3.4 \pm 0.2	0.6 \pm 1.1	81.2	4.2 \pm 0.1	2.1 \pm 0.3	51.3

Note: ND = not detected.

The efficiency of coating the two materials for the concentration of 10^4 CFU/mL reflects higher potential for disinfection than the use of UV-A light alone. Increasing the concentration of bacteria results in reduced antimicrobial activity, since fewer TiO_2 particles are available to each bacterial cell [6,27]. Erdem et al. [56] reported that at concentrations less than or equal to 10^3 CFU/mL, the inhibition rate of bacteria is independent of the initial concentration. The inhibition rate increases for initial concentrations between 10^4 and 10^9 CFU/mL.

3.3.4. Effect of Temperature

There was a significant difference in disinfection after 3 h of treatment for the coated materials at temperatures of 32.3°C and at room temperature of 26°C ($p < 0.01$) (Figure 8). At the higher temperature there was not any significant difference between the two coated materials.

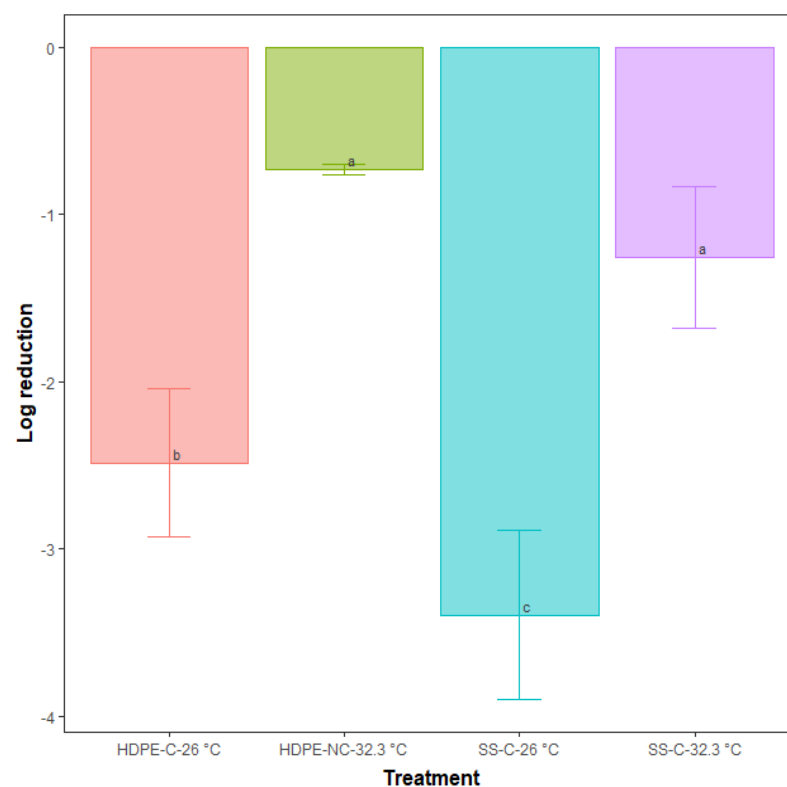


Figure 8. Logarithmic reduction of *E. coli* after 3 h of treatment with the P25 TiO_2 -coated materials with temperature control at 26°C (HDPE-C-F, SS-C-F) and without temperature control at 32.3°C (HDPE-C-NF, SS-C-NF). Error bars represent \pm one standard deviation of three measurements ($n = 3$). Treatments with the same letter are not significantly different ($p > 0.05$).

In the test with temperature control at 26°C , efficiencies above 70% were established after 4.5 h of treatment for materials with coating and only with the presence of UV-A LED light. With a temperature of 32.3°C , the maximum efficiency achieved after 4.5 h was 55.2% for the TiO_2 -coated stainless steel (Figure 8). Dorick et al. [57] described that the optimal growth rate of *E. coli* bacteria is between 30 and 42°C , whereas at lower temperatures, the growth rate is lower. Temperature is a factor affecting disinfection, as reported by Locas et al. [58] when comparing temperatures of 25 and 4°C .

3.4. Identification of TiO_2 Composite Immobilization and the Adhesion Test

An adhesion test was performed for both materials with TiO_2 -based coatings (SS, HDPE) with $n = 9$. A scale adhesion of four was determined, in accordance with the ASTM D3359 (Table 1). The score characterized slight traces of coating removal along the incisions

or at their intersection; however, the coating remained adhered to the substrate with less than approximately 5% coating loss.

TiO₂ agglomerates were formed on the coating surface due to spreading of particles and the curing of resin [40], as shown by the SEM (Figure 9a,b).

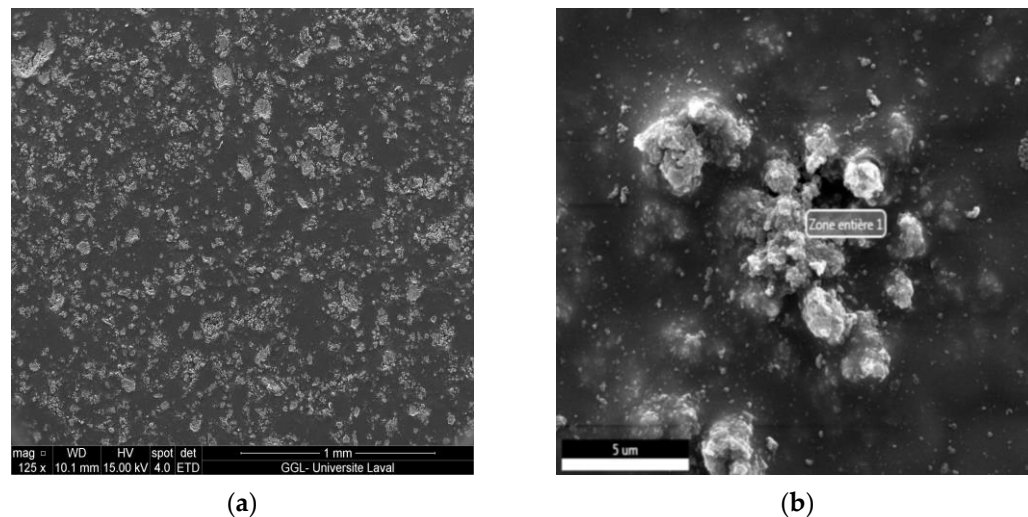


Figure 9. (a) SEM image of SS with a TiO₂-based coating ($\times 125$); (b) SEM image of SS with a TiO₂-based coating ($\times 6000$ magnification).

The detection of TiO₂ on the coating surfaces, as shown in Figure 9b, confirmed the existence of Ti on the TiO₂-coated materials. Additionally, from the EDS analysis for the coating, the amounts of 59.51% of carbon (C), 28.17% of oxygen (O) and 12.32% of titanium (Ti) were determined.

4. Conclusions

In this study, the effects of TiO₂-coated materials and the incidence of UV-A LED light on disinfection were evaluated. The photocatalytic potential of TiO₂-based composites was assessed for selecting the most efficient in the removal of methylene blue (MB) as the redox indicator under the influence of light. Three immobilization methods were studied for coatings with TiO₂-based composites. To select the final immobilization method of TiO₂-based composite, two methods that had the best photocatalytic results in MB degradation were evaluated in a pre-disinfection step.

Two TiO₂-based composites were synthesized in a laboratory (TiO₂, Ag-TiO₂). The TiO₂ composites were compared to a commercial composite, P25 TiO₂, and the best appeared to be the latter one. M2 was the most active for MB degradation. M1 had the best adherence to the materials and performance in the pre-disinfection test.

The coated stainless steel material under UV-A LED light (SS-C-Light) showed the highest inactivation of bacteria: 100% efficiency after 3 h of treatment with no evidence of regrowth at the end of treatment. Polyethylene coated material under UV-A LED light (HDPE-C-Light) had the lowest efficiency with re-growth peaks throughout the test and a maximum removal efficiency of 63.9% in logarithmic reduction. A high initial concentration of bacteria and high temperature reduced the disinfection efficiency of the treatment.

This study evidenced the potential of using TiO₂-coated materials and UV-A LED light (365–390 nm) in the disinfection of a livestock drinking water trough. The combination of UV-A LED/TiO₂ represents an alternative with potential for residual disinfection when compared to the use of UV-A LED light alone. These disinfection techniques should be studied under real-field conditions to evaluate their potential implementation in farms. The synthesis of TiO₂-based composites can be improved by controlling various parameters in the process, such as the method and the compounds, the heat treatment temperature for particle size control and the potential of the particles obtained during photocatalysis in

repeated uses. Finally, the immobilization method should be studied along with the loss of TiO₂-based composites in water.

Author Contributions: Conceptualization, S.F. and S.G.; methodology H.D.P.-R. and J.H.P.; validation, S.F. and S.G.; formal analysis, H.D.P.-R.; investigation, H.D.P.-R.; resources D.C.-M. and S.G.; writing—original draft preparation, H.D.P.-R.; writing—review and editing, H.D.P.-R., S.F., S.G., D.C.-M., C.C., A.N.R. and J.H.P.; visualization, H.D.P.-R. and S.F.; supervision, S.F.; project administration, D.C.-M.; funding acquisition, D.C.-M. and S.G. All authors have read and agreed to the published version of the manuscript.

Funding: This Project titled “Développement de stratégies pour réduire et contrôler des agents pathogènes dans l’eau d’abreuvement dans les élevages vache-veau extérieurs” was funded by the 2018–2019 Innov’ Action agroalimentaire and the partenariat pour l’innovation en agroalimentaire programs under the Canadian Agricultural Partnership between the Ministère de l’Agriculture, des Pêcheries et de l’Alimentation du Québec (MAPAQ) and the Federal Government. We also gratefully acknowledge the financial and technical support from NSERC Discovery Frontiers Program, Université Laval and the Research and Development Institute for the Agri-Environment (IRDA).

Data Availability Statement: Not applicable.

Conflicts of Interest: The authors declare no conflict of interest.

References

1. Olkowski, A.A. *Livestock Water Quality A Field Guide for Cattle, Horses, Poultry and Swine*; University of Saskatchewan: Saskatchewan, Canada, 2009.
2. Beauvais, W.; Gart, E.V.; Bean, M.; Blanco, A.; Wilsey, J.; McWhinney, K.; Bryan, L.K.; Krath, M.; Yang, C.-Y.; Alvarez, D.M.; et al. The prevalence of Escherichia coli O157:H7 fecal shedding in feedlot pens is affected by the water-to-cattle ratio: A randomized controlled trial. *PLoS ONE* **2018**, *13*, e0192149. [[CrossRef](#)] [[PubMed](#)]
3. Chayer, M. Étude de la Qualité de L’eau de Source et D’abreuvement Dans les Élevages Vache-Veau en Fonction des Propriétés Physicochimiques et Bactériologiques. Master’s Thesis, Université Laval, Quebec, QC, Canada, 2021.
4. Davis, R.; Watts, P. *Water trough Design and Sewer Systems. Feedlot Design and Construction*; Meat & Livestock: North Sydney, Australia, 2013.
5. Li, X.; Watanabe, N.; Xiao, C.; Harter, T.; McCowan, B.; Liu, Y.; Atwill, E.R. Antibiotic-resistant, *E. coli* in surface water and groundwater in dairy operations in Northern California. *Environ. Monit Assess* **2014**, *186*, 1253–1260. [[CrossRef](#)]
6. Chen, C.-Y.; Wu, L.-C.; Chen, H.-Y.; Chung, Y.-C. Inactivation of Staphylococcus aureus and Escherichia coli in Water Using Photocatalysis with Fixed TiO₂. *Water Air Soil Pollut.* **2010**, *212*, 231–238. [[CrossRef](#)]
7. Huo, Z.Y.; Du, Y.; Chen, Z.; Wu, Y.H.; Hu, H.Y. Evaluation and prospects of nanomaterial-enabled innovative processes and devices for water disinfection: A state-of-the-art review. *Water Res.* **2020**, *173*, 115–581. [[CrossRef](#)]
8. Upadhyay, P.; Chakma, S. Photocatalytic Water Disinfection. *Appl. Water Sci.* **2021**, *2*, 381–404.
9. Islam, T.; Dominguez, A.; Turley, R.S.; Kim, H.; Sultana, K.A.; Shuvo, M.; Alvarado-Tenorio, B.; Montes, M.O.; Lin, Y.; Gardea-Torresdey, J.; et al. Development of photocatalytic paint based on TiO₂ and photopolymer resin for the degradation of organic pollutants in water. *Sci. Total Environ.* **2020**, *704*, 135406. [[CrossRef](#)] [[PubMed](#)]
10. Chen, Y.-D.; Duan, X.; Zhou, X.; Wang, R.; Wang, S.; Ren, N.-Q.; Ho, S.-H. Advanced oxidation processes for water disinfection: Features, mechanisms and prospects. *Chem. Eng. J.* **2021**, *409*, 128207. [[CrossRef](#)]
11. Hodges, B.C.; Cates, E.L.; Kim, J.H. Challenges and prospects of advanced oxidation water treatment processes using catalytic nanomaterials. *Nat. Nanotechnol.* **2018**, *13*, 642–650. [[CrossRef](#)]
12. Dutta, V.; Singh, P.; Shandilya, P.; Sharma, S.; Raizada, P.; Saini, A.K.; Gupta, V.K.; Hosseini-Bandegharai, A.; Agarwal, S.; Rahmani-Sanie, A. Review on advances in photocatalytic water disinfection utilizing graphene and graphene derivatives-based nanocomposites. *J. Environ. Chem. Eng.* **2019**, *7*, 103132. [[CrossRef](#)]
13. Rao Miditana, S.; Rao Tirukkovalluri, S.; Manga Raju, I.; Bangaru Babu, A.; Ramesh Babu, A. Review on the synthesis of doped TiO₂ nanomaterials by Sol-gel method and description of experimental techniques. *J. Water Environ. Nanotechnol.* **2022**, *7*, 218–229.
14. Prasad, S.; Kumar, V.; Kirubanandam, S.; Barhoum, A. Engineered nanomaterials: Nanofabrication and surface functionalization. *Emerg. Appl. Nanopart. Archit. Nanostruct.* **2018**, 305–340.
15. Liu, N.; Zhu, Q.; Zhang, N.; Zhang, C.; Kawazoe, N.; Chen, G.; Negishi, N.; Yang, Y. Superior disinfection effect of Escherichia coli by hydrothermal synthesized TiO₂-based composite photocatalyst under LED irradiation: Influence of environmental factors and disinfection mechanism. *Environ. Pollut.* **2019**, *247*, 847–856. [[CrossRef](#)] [[PubMed](#)]
16. Liu, N.; Ming, J.; Sharma, A.; Sun, X.; Kawazoe, N.; Chen, G.; Yang, Y. Sustainable photocatalytic disinfection of four representative pathogenic bacteria isolated from real water environment by immobilized TiO₂-based composite and its mechanism. *Chem. Eng. J.* **2021**, *426*, 131217. [[CrossRef](#)]

17. Darbandi, M.; Shaabani, B.; Schneider, J.; Bahnemann, D.; Gholami, P.; Khataee, A.; Yardani, P.; Hosseini, M.G. TiO₂ nanoparticles with superior hydrogen evolution and pollutant degradation performance. *Int. J. Hydrog. Energy* **2019**, *44*, 24162–24173. [CrossRef]
18. Khan, S.; Sadiq, M.; Kim, D.-S.; Ullah, M.; Muhammad, N. TiO₂ and its binary ZnTiO₂ and ternary CdZnTiO₂ nanocomposites as efficient photocatalysts for the organic dyes degradation. *Appl. Water Sci.* **2022**, *12*, 118. [CrossRef]
19. Wang, W.; Ye, M.; He, L.; Yin, Y. Nanocrystalline TiO₂-catalyzed photoreversible color switching. *Nano Lett.* **2014**, *14*, 1681–1686. [CrossRef]
20. Carré, G.; Hamon, E.; Ennahar, S.; Estner, M.; Lett, M.-C.; Horvatovich, P.; Gies, J.-P.; Keller, V.; Keller, N.; Andre, P. TiO₂ photocatalysis damages lipids and proteins in Escherichia coli. *Appl. Environ. Microbiol.* **2014**, *80*, 2573–2581. [CrossRef]
21. Hou, C.; Hu, B.; Zhu, J. Photocatalytic Degradation of Methylene Blue over TiO₂ Pretreated with Varying Concentrations of NaOH. *Catalysts* **2018**, *8*, 575. [CrossRef]
22. Foster, H.A.; Ditta, I.B.; Varghese, S.; Steele, A. Photocatalytic disinfection using titanium dioxide: Spectrum and mechanism of antimicrobial activity. *Appl. Microbiol. Biotechnol.* **2011**, *90*, 1847–1868. [CrossRef] [PubMed]
23. Bogdan, J.; Jackowska-Tracz, A.; Zarzynska, J.; Plawinska-Czarnak, J. Chances and limitations of nanosized titanium dioxide practical application in view of its physicochemical properties. *Nanoscale Res. Lett.* **2015**, *10*, 57. [CrossRef]
24. Islam, M.R.; Parimalam, M.; Sumdani, M.G.; Taher, M.A.; Asyadi, F.; Yenn, T.W. Rheological and antimicrobial properties of epoxy-based hybrid nanocoatings. *Polym. Test.* **2020**, *81*, 106202. [CrossRef]
25. Bertani, R.; Bartolozzi, A.; Pontefisso, A.; Quaresimin, M.; Zappalorto, M. Improving the Antimicrobial and Mechanical Properties of Epoxy Resins via Nanomodification: An Overview. *Molecules* **2021**, *26*, 5426. [CrossRef] [PubMed]
26. Budiprasojo, A.; Budiprasojo, F. Bactericidal Activity of Resin-Titanium Dioxide and Ultraviolet in Killing Escherichia Coli Bacteria. *J. Penerapan Teknol. Dan Pembelajaran* **2021**, *19*, 37–45.
27. Yu, B.; Leung, K.M.; Guo, Q.; Lau, W.M.; Yang, J. Synthesis of Ag-TiO₂ composite nano thin film for antimicrobial application. *Nanotechnology* **2011**, *22*, 115603. [CrossRef] [PubMed]
28. Inrs. Réactions Chimiques Dangereuses, Une Nouvelle Base de Données. 2021. Available online: <https://www.inrs.fr/actualites/reactions-chimiques-dangereuses-nouvelle-base-donnees.html> (accessed on 29 September 2022).
29. Eskandarian, M.R.; Fazli, M.; Rasoulifard, M.H.; Choi, H. Decomposition of organic chemicals by zeolite-TiO₂ nanocomposite supported onto low density polyethylene film under UV-LED powered by solar radiation. *Appl. Catal. B Environ.* **2016**, *183*, 407–416. [CrossRef]
30. Geltmeyer, J.; Teixido, H.; Meire, M.; Van Acker, T.; Deventer, K.; Vanhaecke, F.; Van Hulle, S.; De Buysser, K.; De Clerck, K. TiO₂ functionalized nanofibrous membranes for removal of organic (micro)pollutants from water. *Sep. Purif. Technol.* **2017**, *179*, 533–541. [CrossRef]
31. Al-Ghafri, B.; Lau, W.-J.; Al-Abri, M.; Goh, P.-S.; Ismail, A.F. Titanium dioxide-modified polyetherimide nanofiber membrane for water treatment. *J. Water Process Eng.* **2019**, *32*, 100970. [CrossRef]
32. Dariani, R.S.; Esmaeili, A.; Mortezaali, A.; Dehghanpour, S. Photocatalytic reaction and degradation of methylene blue on TiO₂ nano-sized particles. *Optik* **2016**, *127*, 7143–7154. [CrossRef]
33. Montallana, A.D.S.; Vasquez, M.R. Fabrication of PVA/Ag-TiO₂ nanofiber mats for visible-light-active photocatalysis. *Results Phys.* **2021**, *25*, 104205. [CrossRef]
34. Basumatary, B.; Basumatary, R.; Ramchiary, A.; Konwar, D. Evaluation of Ag@TiO₂/WO₃ heterojunction photocatalyst for enhanced photocatalytic activity towards methylene blue degradation. *Chemosphere* **2022**, *286 Pt 2*, 131848. [CrossRef]
35. İzlen Çifçi, D. Decolorization of methylene blue and methyl orange with ag doped tio2 under UV-a and UV-visible conditions: Process optimization by response surface method and toxicity evaluation. *Glob. NEST J.* **2016**, *18*, 371–380.
36. Lee, D.-S.; Chen, Y.-W. Nano Ag/TiO₂ catalyst prepared by chemical deposition and its photocatalytic activity. *J. Taiwan Instig. Chem. Eng.* **2014**, *45*, 705–712. [CrossRef]
37. Chowdhury, I.H.; Ghosh, S.; Naskar, M.K. Aqueous-based synthesis of mesoporous TiO₂ and Ag-TiO₂ nanopowders for efficient photodegradation of methylene blue. *Ceram. Int.* **2016**, *42*, 2488–2496. [CrossRef]
38. Xu, C.; Rangaiah, G.P.; Zhao, X.S. Photocatalytic Degradation of Methylene Blue by Titanium Dioxide: Experimental and Modeling Study. *Ind. Eng. Chem. Res.* **2014**, *53*, 14641–14649. [CrossRef]
39. Wahab, M.A.; Li, L.; Li, H.; Abdala, A. Silver nanoparticle-based nanocomposites for combating infectious pathogens: Recent advances and future prospects. *Nanomaterials* **2021**, *11*, 581. [CrossRef] [PubMed]
40. Kasanen, J.; Salstela, J.; Suvanto, M.; Pakkanen, T.T. Photocatalytic degradation of methylene blue in water solution by multilayer TiO₂ coating on HDPE. *Appl. Surf. Sci.* **2011**, *258*, 1738–1743. [CrossRef]
41. Yuan, R.; Zheng, J.; Guan, R.; Zhao, Y. Surface characteristics and photocatalytic activity of TiO₂ loaded on activated carbon fibers. *Colloids Surf. A Physicochem. Eng. Asp.* **2005**, *254*, 131–136. [CrossRef]
42. Hussin, M.H.A.; Abdullah, W.R.W.; Awang, M.; Mansor, W.S. Synthesis and characterization of TiO₂/ZnO-epoxy beads and their performance for the degradation of dye. *Univ. Malays. Teren. J. Undergrad. Res.* **2020**, *2*, 9–14. [CrossRef]
43. Shi, X.; Zhang, X.; Ma, L.; Xiang, C.; Li, L. TiO₂-Doped Chitosan Microspheres Supported on Cellulose Acetate Fibers for Adsorption and Photocatalytic Degradation of Methyl Orange. *Polymers* **2019**, *11*, 1293. [CrossRef]
44. Evans, A.; Slate, A.J.; Akhidime, I.D.; Verran, J.; Kelly, P.J.; Whitehead, K.A. The Removal of Meat Exudate and Escherichia coli from Stainless Steel and Titanium Surfaces with Irregular and Regular Linear Topographies. *Int. J. Environ. Res. Public Health* **2021**, *18*, 3198. [CrossRef] [PubMed]

45. Liu, H.; Li, D.; Yang, X.; Li, H. Fabrication and characterization of Ag₃PO₄/TiO₂ heterostructure with improved visible-light photocatalytic activity for the degradation of methyl orange and sterilization of *E. coli*. *Mater. Technol.* **2018**, *34*, 192–203. [[CrossRef](#)]
46. Xie, J.; Hung, Y.-C. Effect of TiO₂ Loading, Water Depth and Light Intensity on Photo-Disinfection Efficacy of Escherichia Coli O157:H7 Using TiO₂ NP-Embedded Cellulose Acetate Film in Water. *Appl. Eng. Agric.* **2021**, *37*, 1–9. [[CrossRef](#)]
47. Sunada, K.; Watanabe, T.; Hashimoto, K. Studies on photokilling of bacteria on TiO₂ thin film. *J. Photochem. Photobiol. A Chem.* **2003**, *156*, 227–233. [[CrossRef](#)]
48. Liu, Y.; Zeng, X.; Hu, X.; Hu, J.; Wang, Z.; Yin, Y.; Sun, C.; Zhang, X. Two-dimensional g-C₃N₄/TiO₂ nanocomposites as vertical Z-scheme heterojunction for improved photocatalytic water disinfection. *Catal. Today* **2019**, *335*, 243–251. [[CrossRef](#)]
49. Bosshard, F.; Riedel, K.; Schneider, T.; Geiser, C.; Bucheli, M.; Egli, T. Protein oxidation and aggregation in UVA-irradiated Escherichia coli cells as signs of accelerated cellular senescence. *Environ. Microbiol.* **2010**, *12*, 2931–2945. [[CrossRef](#)]
50. LeJeune, J.T.; Besser, T.E.; Hancock, D.D. Cattle water troughs as reservoirs of Escherichia coli O157. *Appl. Environ. Microbiol.* **2001**, *67*, 3053–3057. [[CrossRef](#)]
51. Lim, Y.J.; Yoon, J.W.; Hovde, C.J. A Brief Overview of Escherichia coli O157:H7 and Its Plasmid O157. *J. Microbiol. Biotechnol.* **2010**, *20*, 5–14. [[CrossRef](#)]
52. De Vietro, N.; Tursi, A.; Beneduci, A.; Chidichimo, F.; Milella, A.; Fracassi, F.; Chatzisyneon, E.; Chidichimo, G. Photocatalytic inactivation of Escherichia coli bacteria in water using low pressure plasma deposited TiO₂ cellulose fabric. *Photochem. Photobiol. Sci.* **2019**, *18*, 2248–2258. [[CrossRef](#)]
53. Al-Ghanim, K.A.; El-Salam, M.M.A.; Mahboob, S. Assessment of Water Quality for Some Roof Tanks in Alkharj Governorate, KSA. *Pak. J. Zool* **2014**, *46*, 1003–1012.
54. Xiong, P.; Hu, J. Inactivation/reactivation of antibiotic-resistant bacteria by a novel UVA/LED/TiO₂ system. *Water Res.* **2013**, *47*, 4547–4555. [[CrossRef](#)] [[PubMed](#)]
55. Chatzisyneon, E.; Droumpali, A.; Mantzavinos, D.; Venieri. Disinfection of water and wastewater by UV-A and UV-C irradiation. *Photochem. Photobiol. Sci.* **2011**, *10*, 389–395. [[CrossRef](#)] [[PubMed](#)]
56. Erdem, A.; Metzler, D.; Cha, D.; Huang, C.P. Inhibition of bacteria by photocatalytic nano-TiO₂ particles in the absence of light. *Int. J. Environ. Sci. Technol.* **2014**, *12*, 2987–2996. [[CrossRef](#)]
57. Dorick, J.; Hayden, M.; Smith, M.; Blanchard, C.; Monu, E.; Wells, D.; Huang, T.-S. Evaluation of Escherichia coli and coliforms in aquaponic water for produce irrigation. *Food Microbiol.* **2021**, *99*, 103801. [[CrossRef](#)]
58. Locas, A.; Demers, J.; Payment, P. Evaluation of photoreactivation of Escherichia coli and Enterococci after UV disinfection of municipal wastewater. *Can J. Microbiol.* **2008**, *54*, 971–975. [[CrossRef](#)] [[PubMed](#)]